Thermochimica Acta, 104 (1986) 223–245
Elsevier Science Publishers B.V., Amsterdam – Printed in The Netherlands

STUDY OF THE THERMAL BEHAVIOUR OF ORDERED BIMETALLIC EDTA COMPLEXES

E. ESCRIVÁ, A. FUERTES, J.V. FOLGADO, E. MARTÍNEZ-TAMAYO,
A. BELTRÁN-PORTER and D. BELTRÁN-PORTER

Departamento de Química Inorgánica, Facultad de Ciencias Químicas, Universitat de Valencia (Estudi General de València), Burjassot, Valencia (Spain)

(Received 6 January 1986)

ABSTRACT

The study of the thermal behaviour of a family of isostructural ordered bimetallic MM′(EDTA)$\cdot$6H_2O complexes has been performed using TG and DTA. Formal kinetic analysis of the dehydration step has been approached using non-isothermal procedures. The resulting correlation among the calculated E_a values and the cationic sizes implies a common dehydration mechanism. Copper-containing complexes show distinctive behaviour during the ligand pyrolysis processes. A mechanistic interpretation involving formation of Cu(I) and Cu(0) intermediates is furnished. The evolution of the inorganic residues in systems containing both Co and Ni is especially considered given the interest in the $(Co_xNi_{1-x})_{1-y}O$ system.

INTRODUCTION

An extensive family of isostructural bimetallic EDTA complexes having the general stoichiometry MM′(EDTA)$\cdot$6H_2O has been previously described [1,2]. The materials crystallize with the same structure (space group $P2_1na$) as that of Zn_2(EDTA)$\cdot$6H_2O [3] and Co_2(EDTA)$\cdot$6H_2O [4] and can form solid solutions in the range $Mg_\alpha Mn_\beta Co_\gamma Ni_\delta Cu_\epsilon Zn_\phi$(EDTA)$\cdot$6$H_2O$ (where $\alpha+\beta+\gamma+\delta+\epsilon+\phi=2$, $\alpha+\beta\leqslant 1$, $\delta+\epsilon\leqslant 1$, $0\leqslant\epsilon\leqslant 1$, $\phi\leqslant 2$, $0\leqslant\alpha$, $\beta\leqslant 1$). Two roughly octahedral coordination site types can be distinguished in the lattice: M cations occupy the hydrated sites in which they are coordinated to four water molecules and two more *cis*-oxygen atoms belonging to two bridging carboxylate groups of side-EDTA-chelated centres (i.e., they are cationic $(M(H_2O)_4O_IO_{II})^{2+}$ positions); in the chelated anionic sites, M′ cations are six-coordinated to the hexadentate EDTA ligands $(M'(EDTA)^{2-})$. The resulting lattice can be described [2] as formed by zig-zag strings of alternating "hydrated" and "chelated" complex ions linked through carboxylate bridging groups. When dealing with heterobimetallic materials, the lattice shows an "occupational preference" (probably predetermined by the competitive equilibria in solution [2]). "Chelated" and

0040-6031/86/$03.50

"hydrated" sites are occupied selectively by one or the other cation and this results in a regular alternation of both metal atoms in the chains * (i.e., "ordered" heterobimetallic arrangements are obtained).

This type of materials is of interest because of their striking and anomalous anisotropic magnetic properties that have been referred as "ferrimagnetic-like" behaviour [5–8]. The influence on these properties of the synthetic procedure—which may lead to amorphous compounds—has been investigated [9–11] and also it has been possible to change the relative array of the cations using EDTA-like ligands and benefiting from kinetic factors [12–14].

From another point of view, the utilization of solid solution precursors may in some cases constitute an advantageous route (with respect to ceramic or coprecipitation classic procedures) to the synthesis of complex metal oxides [15]. Thus, the metallic elements in these EDTA-derivatives are dispersed but ordered; probably, the relative stoichiometry in the final oxides might be controlled; besides this, their solubility would enable us to deposit them, after impregnation, in appropriate carriers for use in catalytic process reactors. Notwithstanding, previous studies of the thermal decomposition of metal carboxylates already have shown the influence of the starting salt type on the surface specific properties of the pyrolysis products [16,17]. Then, a detailed study on our systems, studying these aspects in depth, might offer significant results. However, it seems clear that such a study (which is now in progress) could be better developed in the light of previous knowledge of the thermal behaviour of the starting complexes. To elucidate this last question constitutes the fundamental aim of the present paper. At the same time, we present preliminary results referring to the evolution of the inorganic degradation residues. The interest is focussed mainly on the $(Co_xNi_{1-x})_{1-y}O$ system given its peculiar electrical and potentially catalytic properties [18].

EXPERIMENTAL

The materials were synthesized and characterized as described previously [1,2].

Thermal analysis was the main technique used to follow the complex evolution. The analyses were made using a Setaram B70 simultaneous TG-DTA thermobalance. Crucibles containing ca. 60 mg of samples were heated at 6.2°C min^{-1} under a dynamic N_2 atmosphere. In the second part of the study, the experiments were performed again in air. The heating rate

---

* Only in the case of $ZnCo(EDTA)\cdot 6H_2O$ are both site types randomly occupied by Zn^{2+} and Co^{2+} [2].

for the kinetic measurements was 0.85°C min^{-1} (sample mass ca. 100 mg). In all cases, calcined Al_2O_3 was used as reference.

Infrared spectra were recorded as nujol and/or fluorolube mulls with a Perkin-Elmer 225 spectrophotometer. For deuteration purposes, the samples were exposed to a D_2O-rich atmosphere in order to induce exchange only for the more labile H_2O molecules.

X-ray powder diffraction patterns were obtained by means of a Kristalloflex 810 Siemens diffractometer using Cu K_α radiation. JCPDF cards were utilized as comparative standards. The apparatus was equipped with a variable temperature device working from room temperature to ca. 1200°C. Distance calculations based on crystal data were performed by means of DISTAN program [19].

Nitrogen microanalyses were done using a Coleman 29-B analyzer; CO and CO_2 in the evolved gas were identified by gas chromatography. Quantitative CO_2 determination was carried out after absorption in a U-shaped tube (attached to the thermobalance gas exit) containing ascarite. This tube was intercalated between two others containing, respectively, $Mg(ClO_4)_2$ (to absorb H_2O vapour) and ascarite (to prevent atmospheric CO_2 entering).

RESULTS AND DISCUSSION

The data set provided by the thermal analysis of the $MM'(EDTA) \cdot 6H_2O$ complexes has been summarized in Table 1. TGA and DTA curves show three different patterns of thermal evolution. Curves in Fig. 1 correspond to compounds whose behaviour is representative of each one of these classes.

Regardless of the ultimate thermal behaviour of each definite product, under the conventional experimental conditions, the occurrence of three consecutive processes, namely, dehydration, ligand pyrolysis and inorganic residue evolution, appears clearly in all cases.

Dehydration

The first process in the thermal evolution of the complexes can be associated with their dehydration. As we shall see, this process, leading to thermally stable materials, is always a complex one. It implies a lowering in the coordination number of the "hydrated" cation [20] and concludes probably with a rearrangement of the EDTA ligand between the two metallic centres.

This dehydration step seems to occur in all cases as a two-stage endothermic process. The weight losses involved correspond to 1 and 5 water molecules, respectively.

TABLE 1

Thermal analysis data for MM'(EDTA)·$6H_2O$ compounds (↑ endo; ↓ exo)

Compound MM' [a]			Dehydration		Ligand pyrolysis			Inorganic residue evolution
			$1H_2O$	$5H_2O$				
	TG [b]		2.5	18.2	35.0			–
MnNi	DTA [c]	s	↑ 46	↑ 100	↑ 364			↑ 450
		p	(84)	142	416			–
	TG		3.1	16.5	31.5			–
ZnNi	DTA	s	↑ 44	↑ 127	↑ 386			↑ 452
		p	(80)	150	406			–
	TG		3.4	17.6	40.1			–
CoNi	DTA	s	↑ 58	↑ 118	↑ 366			↑ 444
		p	(96)	156	426			–
	TG		3.8	17.9	35.0			–
MgNi	DTA	s	↑ 52	↑ 125	↑ 360			↑ 436
		p	(92)	155	422			–
	TG		2.8	17.8	42.3			–
NiNi	DTA	s	↑ 56	↑ 137	↑ 358			↑ 428
		p	(98)	162	420			–
	TG		2.6	17.3	32.5			–
MnZn	DTA	s	↑ 54	↑ 110	↑ 368			420
		p	(86)	150	416			–
	TG		2.5	17.5	32.0			–
ZnZn	DTA	s	↑ 48	↑ 119	↑ 365			↑ 400
		p	(80)	147	496			–
	TG		2.7	17.9	31			9.1
CoZn	DTA	s	↑ 53	↑ 120	↑ 374			↑ 416
		p	(79)	149	406			525
	TG		3.9	19.5	36.0			–
MgZn	DTA	s	↑ 60	↑ 128	↑ 360			↑ 420
		p	(98)	160	418			–
	TG		2.9	17.5	33.0			15.1
MnCo	DTA	s	↑ 58	↑ 106	↑ 358			↑ 404
		p	(90)	152	398			530
	TG		3.5	19.6	32.5			14.4
CoCo	DTA	s	↑ 55	↑ 121	↑ 376			↑ 430
		p	(92)	143	406			500
	TG		4.0	18.9	33.2			14.3
MgCo	DTA	s	↑ 53	↑ 124	↑ 358			↑ 412
		p	(81)	153	394			520
	TG		2.8	17.7	7.0	11.5	24.5	–
MnCu	DTA	s	↑ 50	↑ 108	↓ 230	↓ 276	↑ 350	↑ 496
		p	(90)	134	258	288	384	–
	TG		2.4	18.0	8.0	8.4	27.0	–
ZnCu	DTA	s	↑ 48	↑ 124	↓ 194	↓ 260	↑ 310	↑ 415
		p	(78)	147	230	276	372	–
	TG		3.5	17.4	7.0	9.5	25.0	–

TABLE 1 (continued)

Compound MM′ [a]			Dehydration		Ligand pyrolysis			Inorganic residue evolution
			$1H_2O$	$5H_2O$				
CoCu	DTA	s	↑ 55	↑ 121	↓ 230	↓ 302	↑ 352	↑ 450
		p	(87)	153	244	314	416	–
	TG		4.6	17.7	8.5	11.5	26.0	–
MgCu	DTA	s	↑ 47	↑ 127	↓ 220	↓ 250	↑ 315	↑ 480
		p	(90)	150	240	270	390	–

[a] M = "hydrated" cation $(M(H_2O)_4O_IO_{II})^{2+}$, M′ = "chelated" cation $M(EDTA)^{2-}$.

[b] Percent weight loss.

[c] Temperature (°C); s = process start, p = peak temperature, approximate value is given in parentheses.

The first weight loss can be related with the presence in the crystal lattice of one * water molecule which is essentially isolated. In effect, as mentioned above, all the materials studied here are isostructural with $Zn_2(EDTA) \cdot 6H_2O$ and $Co_2(EDTA) \cdot 6H_2O$. In the case of $Zn_2(EDTA) \cdot 6H_2O$, our calculations based on X-ray diffraction data (performed from the results of Pozhidaev et al. [3]) show the existence of three kinds (structurally distinct) of water molecules **.

(1) Coordination water. Four water molecules (W_1 to W_4) are linked to the metal ion occupying the "hydrated" site. Moreover, they are hydrogen bonded (according to the crystallographic criterion ***) to oxygen atoms from the closest carboxylate (which may belong to adjacent chains) groups.

(2) Lattice water. There is one water molecule (W_5) which is only hydrogen bonded to one oxygen atom from a carboxylate bridge group ($d(W_5–O_b)$ = 3.1 Å) and also to one (W_1) of the coordination water molecules ($d(W_5–W_1)$ = 3.1 Å)

(3) Isolated lattice water. The "sixth" water molecule interacts very weakly with one oxygen atom from the remaining carboxylate bridge ($d(W_6–O_{b'})$ = 3.33 Å) as well as with the mentioned coordination water molecule † ($d(W_6–W_1)$ = 3.36 Å). Both the latter distances are close to the limit established by the crystallographic criterion and it seems reasonable to classify this water molecule as essentially isolated.

---

* In the case of the polycrystalline samples we are working with, this water molecule generally has a non-stoichiometric character (as shown by TG data). This way, the materials might adequately be formulated as $MM'(EDTA) \cdot (5 + x)H_2O$, ($x \leqslant 1$).

** This same conclusion is reached by analysis of the data referred to any of the compounds whose structure has been determined.

*** A hydrogen bond between two neighbouring O atoms is inferred when $d(O \cdots O) \leqslant 3.38$ Å [21].

† This way, this coordination water molecule (W_1) has a distinctive character.

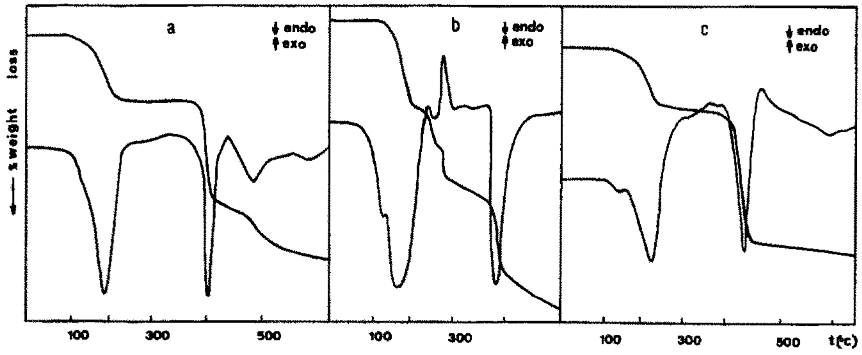

Fig. 1. TG–DTA plots for selected compounds (dynamic nitrogen atmosphere, 6.2°C min^{-1}): (a) $Co_2(EDTA)\cdot 6H_2O$ representative of the series $MCo(EDTA)\cdot 6H_2O$ (M = Mg, Co, Zn, Mn); (b) $MnCu(EDTA)\cdot 6H_2O$, representative of the series $MCu(EDTA)\cdot 6H_2O$ (M = Hg, Co, Zn, Mn); (c) $Ni_2(EDTA)\cdot 6H_2O$, representative of the remaining compounds studied.

Dealing with the materials for which there lacks a direct structural proof, the isolated character of this molecule must be elucidated through alternative ways. In this sense, even though not definitive [22], the isostructurality of the compounds, as well as the low values of the first-dehydration temperatures (Table 1) and their corresponding activation energies (Table 2) are factors supporting it.

The evidence provided by IR spectroscopy is more significant; in all cases, a broad and complex band appears between 2800 and 3700 cm^{-1}. The main component of this band shows a maximum close to 3400 cm^{-1}, clearly assignable to OH group (of hydrogen bonded water molecules) stretching vibrations. However, there are also two sharp absorptions at 3615 and 3480 cm^{-1}, whose assignment is not immediate, given their relatively high values. Notwithstanding, it is a well known fact of the existence of an inverse relation between the values of $\nu_{\text{stretching}}(OH)$ and the strength of a hydrogen bond involving this group. The following relations have been established both empirically and theoretically [21,23]:

$$k_{OH} = 4\pi^2 \mu c^2 \nu_{OH}^2$$

$$r_{OH} = 0.335 + \left(1.86 \times 10^5 / k_{OH}\right)^{1/3}$$

$$\Delta H = 42.9 - 0.0114\nu_{OH}$$

k_{OH} being the strength constant of the OH bond, r_{OH} the bond length, ΔH the enthalpy of the hydrogen bond in kcal mol^{-1}, $c = 2.998 \times 10^{10}$ cm s^{-1} and μ the reduced mass of the OH group (1.562×10^{-24} g).

When these equations are applied for the ν values of the observed sharp absorptions *, results in Table 3 (which includes, for comparison, some

---

* Regardless of the cations nature, these ν values are identical (within experimental error) for all the studied complexes.

TABLE 2

Activation energies (kcal mol^{-1}) for
(1) $MM'(EDTA)\cdot 6H_2O(s) \rightarrow MM'(EDTA)\cdot 5H_2O(s) + H_2O(g)$
(2) $MM'(EDTA)\cdot 5H_2O(s) \rightarrow MM'(EDTA)\cdot 2H_2O(s) + 3H_2O(g)$

Hydrated cation $(M(H_2O)_4O_IO_{II})^{2+}$	Chelated cation $(M'(EDTA)^{2-})$											
	Zn			Co			Ni			Cu		
	$E_a(1)$	$E_a(2)$ [a]	$E_a(2)$ [b]	$E_a(1)$	$E_a(2)$ [a]	$E_a(2)$ [b]	$E_a(1)$	$E_a(2)$ [a]	$E_a(2)$ [b]	$E_a(1)$	$E_a(2)$ [a]	$E_a(2)$ [b]
Mn	13	32	26	12	31	25	14	33	21	13	22	19
Zn	12	43	36	13	40	31	12	42	38	13	40	34
Co	11	39	31	11	41	33	12	43	37	12	41	33
Mg	12	46	37	9	47	35	10	45	40	11	46	39
Ni	–	–	–	–	–	–	10	49	41	–	–	–

[a] Abou-Shaaban and Simonelli's procedure [27].

[b] Satava's procedure [28]; random nucleation model.

TABLE 3

Hydrogen bond parameters

Compound	ν_{OH}(cm^{-1})	k(dine cm^{-1})	r_{OH}(Å)	ΔH(kcal mol^{-1})
MM′(EDTA)·$6H_2O$	3615	7.27×10^5	0.970	1.63
	3475	6.75×10^5	0.986	3.11
$Na_2(Fe(CN)_5NO)\cdot2H_2O$	3608	7.22×10^5	0.971	1.77
	3570	7.07×10^5	0.971	2.20
$CaSO_4\cdot2H_2O$	3500	6.79×10^5	0.984	3.00
$MgCl_2\cdot4H_2O$	3440	6.56×10^5	0.992	3.68

literature data referred to other crystalline hydrates) are calculated. The k_{OH}, r_{OH} and ΔH values obtained for the complexes suggest that the absorption at 3615 cm^{-1} must be assigned to stretching vibrations of OH groups belonging to isolated (and weakly hydrogen bonded) water molecules like those described for $Na_2Fe(CN)_5NO\cdot2H_2O$. On the other hand, the absorption at 3475 cm^{-1} should be assigned to $\nu_{stretching}$(OH) in non-isolated (and implied in hydrogen bonds of moderate strength) water molecules as occurs in $MgCl_2\cdot2H_2O$ and $CaSO_4\cdot4H_2O$ [21].

In an attempt to corroborate this interpretation, samples of MgNi(EDTA) $\cdot 6H_2O$, MgZn(EDTA) $\cdot 6H_2O$ and Zn_2(EDTA) $\cdot 6H_2O$ were deuterated and their IR spectra recorded. In all three cases, the absorptions at 3615 and 3475 cm^{-1} are missing in the spectra now registered, whereas the main broad component remains but its maximum is shifted slightly to 3300 cm^{-1}. At the same time, a new complex band appears between 2300 and 2700 cm^{-1} with maxima at 2410 and 2500 cm^{-1} and weaker components at 2350 and 2690 cm^{-1}. According to the literature [21], the absorptions near to 2410 and 2500 cm^{-1} can be assigned to stretching vibrations of D–O bonds of water molecules which participate in hydrogen bonds of moderate intensity. The absorption at 2690 cm^{-1} must correspond to $\nu_{stretching}$(D–O) of essentially isolated water molecules. The absorption at 2350 cm^{-1} can be attributed to the harmonic 2 δ (DOD). In short, these assignments indicate that there are two kinds of deuterated water molecules which must correspond with the water molecules of the complexes originating the 3615 and 3475 cm^{-1} frequencies. So, it is reasonable to identify them as W_6 and W_5, respectively. Lastly, the permanence of the main band (3200–3500 cm^{-1}) must be due to the absence of deuteration of the coordination water molecules.

Once the weakness of the forces linking the "sixth" water molecule to the crystal lattice of the MM′(EDTA) $\cdot 6H_2O$ complexes is understood, its non-stoichiometric character (in polycrystalline samples), the low temperature at which it is removed and the low activation energy required, can be explained.

A survey of the conventional TGA curves does not allow accurate inference of the apparition of stable intermediates in the course of the second stage of the dehydration (MM′(EDTA) · $5H_2O \rightarrow$ MM′(EDTA)). Nevertheless, Logvinenko et al., by application of a quasi-isothermal heating programme under quasi-isobaric conditions, detected the formation of di- and mono-hydrate intermediates in the case of some MgM(EDTA) · $6H_2O$ compounds [24]. In this sense, we have also reported [2] spectroscopic evidence showing the tetracoordination of the initially "hydrated" cation (M) in partially dehydrated materials having the general stoichiometry MM′ (EDTA) · $2H_2O$.

This way, it seems reasonable to assume that the second dehydration stage is actually a step by step process that might be schematically written as: MM′(EDTA) · $5H_2O \xrightarrow{1}$ MM′(EDTA) · $2H_2O \xrightarrow{2}$ MM′(EDTA) · $H_2O \xrightarrow{3}$ MM′(EDTA). The first step would imply the elimination of the remaining lattice water (W_5) and two of the coordination water molecules. The coordination around the "hydrated" site would change from distorted octahedral to tetracoordinate, whereas the "chelated" site would stay practically unaltered. Then, the formation of the anhydrous materials will probably involve a deep rearrangement of the EDTA-metal bonds.

To gain further insight into the consequences of the occupational preference for the two coordination sites in the crystalline structure, we approached the study of the formal kinetics of the reaction MM′(EDTA) · $5H_2O \rightarrow$ MM′(EDTA) · $2H_2O$. This is very likely to be single step. Accordingly, its non-isothermal kinetic analysis can offer significant kinetic parameter values * [25]. Before discussing the results, a short comment on the temperature of the process shall be given. So, it can be seen from Table 1 that, for a series in which the "hydrated" cation (M) is the same, this dehydration temperature (t_s and/or t_p) does not vary appreciably. On the other hand, for a given "chelated" cation (M′), a monotonous increase can be observed in the temperatures as the radius of the "hydrated" M^{2+} cation lessens (that is to say, t varies in the order $\mathrm{Mn} < \mathrm{Zn} \leqslant \mathrm{Co} < \mathrm{Mg} < \mathrm{Ni}$). Bearing in mind the isostructurality of the materials, this correlation in the dehydration temperature might be significant if the reaction mechanism were the same.

The values of the kinetic parameters listed in Table 2 have been determined using the mathematical approach of Abou-Shaaban and Simonelli (thus obviating the actual nature of the formal mechanism) [27]. The following observations can be made from the tabulated values: (1) as expected, the calculated activation energies are markedly higher than those corresponding to the "isolated" water molecule removal, (2) for a given "hydrated" cation

---

* The study of the total process (MM′(EDTA)·$5H_2O \rightarrow$ MM′(EDTA)) requires the application of isothermal procedures [26]. Even so, the complexity and probable counterposition of the factors involved would hinder the extraction of unambiguous conclusions from it.

(M), the activation energy of the reaction is practically independent of the "chelated" cation (M′) nature and (3) in a series of complexes having the same "chelated" cation (M′), there is good correlation between the calculated E_a and the nature of the "hydrated" cation (M). This correlation coincides with that observed for the dehydration temperatures. A plot of E_a vs. $1/r(M^{2+})$ (or vs. the ionic potential) leads to a nearly linear relationship).

Whereas the constancy of E_a for a given cation M fully agrees with the above considerations on the structural character of the water molecules involved, the pointed correlation enables us to make the following statements: (1) since we are studying the same total reaction referred to isostructural starting materials, the correlation among the E_a values must imply a common dehydration mechanism and (2) if this is so, the fact that both dehydration temperature and the E_a value can be related with the ionic potential of the "hydrated" cation indicates (a) an essentially ionic component in the metal to coordination water interactions * and (b) that the breakdown of these bonds could probably be the rate controlling step.

According to the conclusions of previous works [25,26], we can use the calculated values of the kinetic parameters as reference criteria for elucidation of the formal dehydration mechanism type by non-isothermal procedures (applied to the same data set). We have utilized Satava's integral method [28] to analyze the more widely assumed models for the kinetic study of solid state reactions [29].

In general, it can be said: (1) the assayed models corresponding to a diffusion mechanism lead systematically to kinetic parameter values close to, but high compared with those above; (2) the phase boundary models also give grouped, but very low values; (3) the nuclei growth models provide dispersed values that fall between those corresponding to diffusion and phase boundary mechanisms. In a systematic way, those corresponding to a random nucleation model are far closer to those obtained by means of the Abou-Shaaban and Simonelli procedure **.

Thus, a nuclei growth formal mechanism can be assumed for the dehydration process. Really, in line with foregoing considerations, it is not surprising that, in the case of a relatively open structure like that dealt with here, the

---

* As it can be noted (see Table 2), the variation in the E_a values for the removal of the "sixth" water molecule follows the opposite order to that now observed. Taking into account that the strength of a hydrogen bond linking W_6 to the coordination water molecule (W_1) will vary inversely with that of the $M-OH_2$ bonds, both correlations become satisfactorily consistent.

** The E_a values corresponding to a one-dimensional phase boundary mechanism have been reported previously [2]. In effect, these values are too low. The correlation among the E_a values was then mentioned but this correlation is observed for all the assayed models. We have shown before [25] that the criterion used there to propose the more likely mechanism by non-isothermal procedures (that leading to the best fit) may lead to erroneus conclusions.

nuclei growth could be the rate controlling step (given that the apparition of active nuclei requires probably the breakdown of M–OH_2 bonds).

Ligand pyrolysis

The literature contains a great deal of information about EDTA degradation in simple complexes [30–35]. However, the complexity of the process (which generally involves two overlapping steps, namely decarboxylation (in one or more stages) and breakdown of the ethylendiamine structure) and the great diversity of possible products preclude exhaustive interpretations [36]. In our case, the appearance of a new structural feature, as is the sharing of carboxylate groups between "hydrated" and "chelated" cations, may introduce additional difficulties.

After the stability interval following the dehydration (ca. 240–360°C), all the complexes studied here undergo the ligand pyrolysis.

Except for the copper containing complexes (which, given their singularity, will be considered below) this process appears in the thermograms as a unique endothermic stage (see Table 1). The temperature range in which it is observed allows one to consider three generic reaction schemes as the most reasonable to "describe" the process:
(A) $MM'(EDTA)(s) \rightarrow MCO_3(s) + M'CO_3(s) + R(g)$
(B) $MM'(EDTA)(s) \rightarrow MO(s) + M'CO_3(s)$ (or $MCO_3(s) + M'O(s)$) $+ R(g)$
(C) $MM'(EDTA)(s) \rightarrow MO(s) + M'O(s) + R(g)$
where R(g) stands for the evolved gas(es).

The theoretical weight losses accompanying these "reactions" have been summarized in Table 4. As can be observed, the experimental weight loss corresponds in most cases ($M = Mg$, Mn or Zn and $M' = Co$, Ni or Zn, and $M = Co$ and $M' = Co$) to a type (A) process (carbonates formation). Notwithstanding, the experimental percentages for MNi(EDTA) ($M = Co$ or Ni) and also for MCu(EDTA) ($M = Zn$, Co, Mg or Mn) fit better to oxide and carbonate formation (type (B) process). Thus, it is reasonable to assume the occurrence of at least two possible pathways for the pyrolysis reactions.

In any case, the formation of carbonates requires partial EDTA decarboxylation. Really, this is the starting step in the degradation of simple EDTA complexes. So, as shown by Charles [36] and by Bhat and Krishna [32], the initially evolved gases contain CO_2 and CO. Decarboxylation can proceed in a unique stage (Sb, Cu, Ni) or in several stages (Ca, Ba, Co) [32]. This last fact suggests that, in the degradation process, Co^{2+} displays higher affinity towards the carboxylate groups than Cu^{2+} and Ni^{2+} (which agrees with the relative thermal stability of the carbonates; decomposition temperatures of crystalline compounds (°C) are: Mg, 600; Mn, 560; Zn, 520; Co, 450; Cu, 400; Ni, 370 [37,38]). In our case, the sharing of carboxylate groups very likely implies a competition between the two structural types of cations and the decarboxylation mechanism must be, if not controlled, at least in-

TABLE 4

Theoretical and experimental weight losses for the ligand pyrolysis process

Compound		Δm%		
MM′(EDTA)·$6H_2O$	Exp [a]	A [b]	B [c]	C [d]
MnNi	44.1	41.9	53.2	64.1
ZnNi	38.6	40.8	52.3	63.1
CoNi	50.0	41.4	53.0	63.0
MgNi	44.9	45.3	57.1	69.0
NiNi	52.2	41.4	53.0	63.1
MnZn	39.9	41.2	51.9	62.7
ZnZn	39.5	40.2	51.1	61.0
CoZn	38.2	41.4	52.3	63.1
MnCo	40.2	41.9	53.2	64.1
CoCo	40.4	41.4	53.0	63.0
MgCo	45.6	45.3	57.1	69.0
MnCu	52.4	41.4	52.2	63.0
ZnCu	50.3	40.3	50.8	61.4
CoCu	49.5	40.9	51.6	62.4
MgCu	59.0	44.7	56.4	68.1

[a] Referred to anhydrous MM′(EDTA) materials.

[b] $MM'(EDTA)(s) \rightarrow MCO_3(s) + M'CO_3(s)$.

[c] $MM'(EDTA)(s) \rightarrow MCO_3(s) + M'O(s)$ (or $MO(s) + M'CO_3(s)$).

[d] $MM'(EDTA)(s) \rightarrow MO(s) + M'O(s)$.

fluenced by the nature of both. In this sense, it can be reasonably assumed that, after dehydration, the carboxylate bridge groups will become more strongly attached than before to the "hydrated" cations (to lessen the effect of the coordination water lost); this probably implying a relative increase in thermal lability for the monodentate carboxylate groups.

This way, the nature of the "chelated" cation may be the main factor in the control of the pyrolysis results. When this cation forms a relatively unstable carbonate, monodentate carboxylates could constitute the first gas evolved in the form of CO_2. The cation would be stabilized as an oxide (ceasing in the competition for the bridge groups) and, after breakdown of the ethylendiamine skeleton, the inorganic residue would contain a mixture of the carbonate of the "hydrated" cation (which would retain the bridge groups) and the oxide of the "chelated" one. As shown below, this "mechanism" has been fully corroborated for the copper complexes and there also exist structural supporting evidence for CoNi(EDTA)·$6H_2O$ and NiNi(EDTA)·$6H_2O$.

On the contrary, if the "chelated" cation gives rise to a more stable carbonate, it is probable that only a fraction of the monodentate groups be eliminated. The gas initially evolved would be essentially CO and the inorganic residue would be composed of only carbonates.

At this point, only Ni^{2+} seems to be peculiar given that the pyrolysis process type varies with the nature of the "hydrated" cation. Thus, unlike the above-mentioned $CoNi(EDTA) \cdot 6H_2O$ and $NiNi(EDTA) \cdot 6H_2O$ cases, the pyrolysis of the remaining compounds in the series $MNi(EDTA) \cdot 6H_2O$ (i.e., for M = Mg, Mn and Zn) yields only carbonates. It may be significant that these last three cations are spherical (d^0, d^5 and d^{10}, respectively) and that their carbonates are the most stable among those considered here. The tendency of this type of cation to yield carbonates by decomposition of homo-bimetallic $M_2(EDTA) \cdot xH_2O$ salts is clear. Thus, in complexes like $Mg_2(EDTA) \cdot 9H_2O$ (lacking even carboxylate bridges) "both" cations ("hydrated" and "chelated") form the carbonate after pyrolysis [35] This fact suggests an electrophilic attack of the carboxylate C=O double bonds by the M^{2+} cations. In the present case, the presence of carboxylate bridge groups would render that attack unnecessary and the initial formation of carbonate by the part of the "hydrated" cation could act synergically on the "chelated" one, in this way avoiding its total (CO should be evolved) decarboxylation (that, in other words, could have been relatively easy). This alternative way would lead also (as observed) to a type (A) process *.

Degradation mechanism of $MCu(EDTA) \cdot 6H_2O$ complexes

Curve b in Fig. 1 is representative of the thermal evolution of $MCu(EDTA) \cdot 6H_2O$ complexes (M = Mg, Co, Zn, Mn). Data in Table 5 have been obtained by thermal analysis of isostructural $M_{1+x}Cu_{1-x}(EDTA) \cdot 6H_2O$ solid solutions; these show TG–DTA curves similar to b.

As mentioned above, after dehydration, the thermal evolution of the copper containing complexes is peculiar in present context. So, the ligand pyrolysis processes do not now arise as a unique endothermic stage on TG–DTA curves but two exothermic steps appear preceding to one endothermic effect. The weight losses associated with each of these steps are summarized in Tables 1 and 5.

By analogy with observations of related compounds ($Na_2Cu(EDTA) \cdot 3.5H_2O$ [31], $H_2Cu(EDTA) \cdot H_2O$ [32], $Cu_2(EDTA) \cdot 4H_2O$ [39]), the intermediate exothermic steps could correspond with decarboxylation reactions. It can readily be shown that the extent of this possible decarboxylation is quantitively related with the presence of Cu^{2+} in the complex. Thus, a plot of Δm (total percent weight loss in both steps) vs. the copper content of the complex (%) shows a clear linear dependence. This fact indicates that the

---

* Probably, this is the way through which all the compounds undergo pyrolysis (excepting copper complexes, see below) having Mg, Mn or Zn as "hydrated" cations. However, the results would be the same whether the initial formation of the "hydrated" cation carbonate induces that of the "chelated" carbonate or if the stabilization of the "chelated" cation carbonate (from monodentate carboxylate groups) leaves the bridge groups at liberty to interact with the "hydrated" cation to yield carbonate.

TABLE 5

Thermal analysis data for $M_{1+x}Cu_{1-x}(EDTA)\cdot 6H_2O$ compounds (↑ endo; ↓ exo)

Compound			Dehydration		Ligand pyrolysis			Inorganic residue evolution
			$1H_2O$	$5H_2O$				
$Zn_{1.8}Cu_{0.2}$	TG [a]		2.3	17.0	3.8		28.0	–
	DTA [b]	s	52	116	240		362	420
		p	↑ (84)	↑ 151	↓ 310		↑ 398	–
$Zn_{1.5}Cu_{0.5}$	TG		2.4	17.1	4.0	5.0	27.0	–
	DTA	s	55	120	254	310	374	430
		p	↑ (82)	↑ 158	↓ 266	↓ 324	↑ 386	–
$M_{1.55}Cu_{0.45}$ [c]	TG		2.7	16.9	3.5	5.0	29.5	–
	DTA	s	52	115	266	320	370	445
		p	↑ (78)	↑ 143	↓ 284	↓ 334	↑ 382	
$Co_{1.35}Cu_{0.65}$	TG		2.9	17.6	4.5	6.0	24.5	–
	DTA	s	60	125	266	320	370	440
		p	↑ (84)	↑ 151	↓ 284	↓ 334	↑ 382	–

[a] Percent weight loss.

[b] Temperature (°C); s = process start, p = peak temperature, approximate value given in parentheses.

[c] Pentametallic compound $Mg_{0.36}Co_{0.40}Zn_{0.38}Ni_{0.41}Cu_{0.45}$.

total process corresponds to a general decomposition reaction that can be written as

$$M_{1+x}Cu_{1-x}(EDTA)(s) \rightarrow M_{1+x}Cu_{1-x}Z(s) + (1-x)X(g)$$

where Z is an unknown organic and X a gas or a gaseous mixture.

The "average mass-formula" of X can be easily determined based on its equivalence with the reduced (i.e., referred to 1 mol of Cu^{2+}) weight loss values, ΔM ($\Delta M = \Delta m M_f/100(1-x)$, M_f standing for the mass-formula of $M_{1+x}Cu_{1-x}(EDTA)\cdot 6H_2O$). ΔM values have been summarized in Table 6. The average value, 90 ± 3 g mol^{-1}, fits the loss of two $-CO_2$ groups.

TABLE 6

Reduced weight losses

Compound	% Cu	Δm%	ΔM
$Zn_{1.8}Cu_{0.2}(EDTA)\cdot 6H_2O$	2.4	3.5	86
$M_{1.55}Cu_{0.45}(EDTA)\cdot 6H_2O$	5.2	8.5	90
$Zn_{1.5}Cu_{0.5}(EDTA)\cdot 6H_2O$	6.3	9.0	92
$Co_{1.35}Cu_{0.65}(EDTA)\cdot 6H_2O$	7.9	10.5	85
$ZnCu(EDTA)\cdot 6H_2O$	12.1	16.4	86
$CoCu(EDTA)\cdot 6H_2O$	11.6	16.5	89
$MnCu(EDTA)\cdot 6H_2O$	12.3	18.5	92
$MgCu(EDTA)\cdot 6H_2O$	13.1	20.0	96

TABLE 7

Analytical quantitative determination

Compound	CO_2 in evolved gas			N in residue	
	m(mg) of sample	mCO_2 (mg)	$nCO_2/nCu(II)$	m_N (calc)	m_N (found)
$MnCu(EDTA)\cdot 6H_2O$	70.37	8.4	1.4	5.6	5.8
$MgCu(EDTA)\cdot 6H_2O$	58.77	7.4	1.5	3.7	3.8
$CoCu(EDTA)\cdot 6H_2O$	97.46	10.4	1.5	5.4	5.2
$Zn_{1.5}Cu_{0.5}(EDTA)\cdot 6H_2O$	108.93	7.6	1.6	3.4	3.4

Qualitative chromatographic analyses show that the evolved gas, X, contains CO_2 in higher proportion than CO as well as traces of O_2. Quantitative determination of the evolved CO_2 was carried out, as described in Experimental, the heating was stopped after the second exothermic step; results are listed in Table 7. As can be observed, the average value of the molar CO_2/Cu^{2+} ratio is 1.5 ± 0.1, this being consistent with a molar CO_2/CO relation 3/1 in the evolved gas. In parallel, the N content in the resulting residue was determined by elemental analysis (see Table 7). All the initial N remains in the residue. This way, the EDTA ethylendiamine portion results appear thermally more stable than two of the carboxylate groups whose elimination must then be associated with the observed exothermic effects.

On the other hand, IR spectra of all the partially decarboxylated materials lack the 1380 cm^{-1} band which is clearly assignable, in the starting $MCu(EDTA)\cdot 6H_2O$ complexes, to the symmetric stretching vibration of monodentate carboxylate groups [2]. This fact, agreeing with foregoing observations, suggests that the removed carboxylate groups are exclusively those coordinated to only Cu^{2+} (i.e., the "chelated" cation).

Once the nature of the exothermic steps is established *, its more probable mechanistic interpretation seems relatively simple and has been schematized in Fig. 2. The first decarboxylation step very likely involves a monoelectronic transference from a monodentate $-CO_2$ group to the Cu^{2+} "chelated" cation which would then become reduced to Cu(I). At the same time, the homolytic breakdown of the $R-CO_2$ bond would liberate a mole of CO_2. On the other hand, the subsequent (second step) formation of CO_2 and CO (in an equimolar relation) can be explained based on the concerted action of two parallel processes. One of them, similar to the former, would yield Cu(0) and CO_2. In the other (which would involve the remaining Cu(I) half), the electronic transference would occur in the inverse sense (i.e., from Cu(I) to the donor oxygen atom of the monodentate group). Then, the

---

* According with thus far stated, the endothermic step concluding the pyrolysis process would imply the evolution of $M_{1+x}Cu_{1-x}Z(s)$ until a mixture containing oxide and carbonate was obtained.

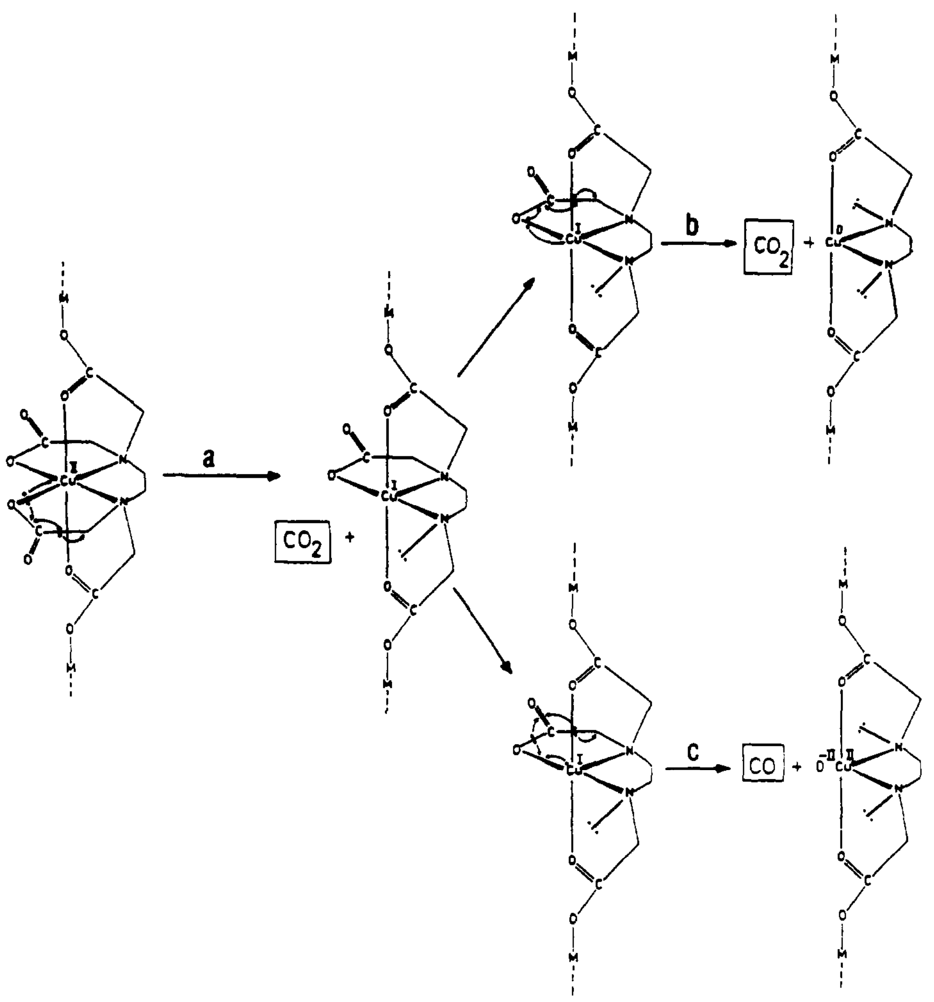

Fig. 2. Schematic representation of the proposed degradation mechanism for MCu(EDTA)·6H_2O complexes (the arrows indicate the sense of the electronic transference). (a) $MCu^{II}(EDTA)(s) \rightarrow CO_2(g)+MCu^{I}Y(s)$; Cu(II) is reduced to Cu(I) and 1 mole of CO_2 per Cu mol is evolved. (b) $1/2MCu^{I}Y(s) \rightarrow 1/2CO_2(g)+1/2MCu^{0}Y'(s)$; half of Cu(I) is again reduced; an equimolecular amount of CO_2 is evolved. (c) $1/2MCu^{I}Y(s) \rightarrow 1/2CO(g)+1/2MCu^{II}Y''(s)$; half of Cu(I) is oxidized to give a CuO precursor; an equimolecular amount of CO is evolved. Overall process: $MCu^{II}(EDTA)(s) \rightarrow 3/2CO_2(g)+1/2CO(g)+MCuZ(s)$ $(1/2MCu^{0}Y'(s)+ +1/2MCu^{II}Y''(s))$.

homolytic breakdown of R–CO_2 and C–O bonds would liberate CO yielding a CuO precursor species. The very reactive Cu(0) centres generated will be oxidized easily in the ultimate endothermic step * and should be detected

---

* The unaffected carboxylate bridge groups contain enough oxygen to oxidize it to form the "hydrated" cation carbonate.

as the oxide in the residue. The "hydrated" cation, without the Cu^{2+} competition for the bridge groups, would then form carbonate. It must be pointed out that the formation of Cu(I) intermediates has been recognized in the course of the thermal degradation of some simple Cu(II) carboxylates (which may lead also to Cu(0) as end product in N_2 atmosphere) [7].

Although this probable mechanism accounts for the experimental data, it seems necessary to offer a reasonable explanation about the origin of this distinctive behaviour.

The tendency of Cu(II) to acquire square planar coordination is well known, as well as the severe tetragonal distortions from octahedral symmetry shown by many other of its complexes (as a consequence of the Jahn–Teller effect). Often, these distortions are so great that Cu-axial ligand bond distances are referred to as semi-coordination distances [40].

In the anionic moiety of $MnCu(EDTA) \cdot 6H_2O$, $(Cu(EDTA))^{2-}$, (whose structure has been resolved [41]), there is, in effect, a significant difference among the $Cu{-}O_{equatorial}$ (from monodentate carboxylate) and $Cu{-}O_{axial}$ (from bridge carboxylate). average distances, the latter being appreciably longer than the former (2.00 ± 0.02 Å vs. 2.25 ± 0.03 Å, respectively). On the other hand, although all the carboxylate groups in EDTA and EDTA-like Cu(II) coordination compounds are asymmetric (i.e., their C–O bonds are not equivalent), X-ray diffraction data (when they are known) as well as $\nu_{stretching}$ (COO) vibration frequency values [1,2], indicate that the multiplicity of the $C{-}O_{donor}$ bond is higher in the axial bridge groups than in equatorial monodentate ones. This way, the carboxylate bridge groups should have a semi-coordinate character with respect to Cu(II). This is the main difference among the copper containing complexes and others studied here (i.e., in the latter, the coordination polyhedron around the "chelated" cation does not show any appreciable departure among the M–O bond distances [3,4,8,41]. So, the comparatively raised covalence of the $Cu{-}O_{equatorial}$ bonds will be a factor whose influence on the destabilization of the carboxylate linked group is well known [17]. Additionally, it has also been proven that, in EDTA-like complexes, the equatorial rings are more strained than the axial ones [13].

The resulting distinctive destabilization for the monodentate carboxylate groups in the copper containing complexes could then explain their selective removal in the initial pyrolysis steps.

STUDY IN AIR ATMOSPHERE

Experiments analogous to that reported above have been carried out replacing the N_2 flux by a controlled air atmosphere in the muffle. TG–DTA curves plotted in Fig. 3 correspond to the same compounds of that in Fig. 1.

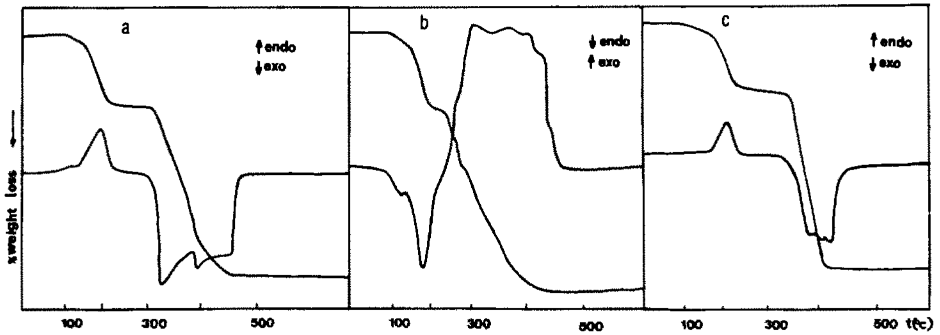

Fig. 3. TG–DTA plots for selected compounds (in air, 6.2°C min^{-1}): (a) $Co_2(EDTA)\cdot 6H_2O$; (b) $MnCu(EDTA)\cdot 6H_2O$; (c) $Ni_2(EDTA)\cdot 6H_2O$.

In this case, only two general types of thermal behaviour are observed. Whereas the copper containing complexes maintain their peculiar behaviour in the decarboxylation steps, there is no apparent difference in the way in which the pyrolysis residues evolve.

As a generalization, it can be said that all three processes in the course of the complex degradation (dehydration, ligand pyrolysis and residue decomposition) occur at lower temperatures than in N_2 atmosphere. In the same way, DTA curves now show a greater complexity (mainly associated with the pyrolysis process).

The same correlations established for the activation energies of the dehydration stages in the foregoing study have been found again, thus supporting the conclusions thus reached. The fact that the ligand pyrolysis starts now at lower temperature is a reasonable consequence of the lower stability of the complexes versus combustion. The process is complex but, as should be expected, exothermic when considered as a whole. Although in several cases there is a change in the TG curve slope during pyrolysis (the initial weight loss being probably associated with carbonate formation), the total weight loss in this process corresponds well with monoxide formation as end products (except for the complexes containing Co(II) or Mn(II) whose pyrolysis would yield mainly Co_3O_4 and Mn_2O_3, respectively).

Inorganic residue evolution

As mentioned above, the understanding of the evolution which the inorganic residue undergoes (carbonate or oxide plus carbonate under N_2 atmosphere and oxides under air atmosphere) after the ligand pyrolysis is required for the subsequent study on its surface specific properties and on those of the final products. For these reasons, our interest here is focussed mainly on the complexes containing both Co and Ni.

Returning to the behaviour in N_2 atmosphere, TG–DTA curves show that, immediately following ligand pyrolysis, (see Table 1) the decomposition of the residual solid mixture commences (carbonate or oxide plus carbonate). The presence of carbonate in the mixtures was chemically demonstrated in all cases by spot tests [42]. However, X-ray diffraction patterns correspond generally (under these working conditions; see below) to poorly-crystalline or even non-crystalline phases. This is not striking and the literature shows that amorphous solids obtained via decomposition of complex salts can be precursors of crystalline phases [43].

Accordingly, the endothermic evolution is observed in most cases as a continuous process (within the temperature range considered) without sharp accidents on DTA curves and is accompanied by a smooth and gradual weight loss (that, in general, ends near 900°C).

So, it results in the peculiar behaviour of the complexes containing initially Co(II) in the "chelated" site. For these compounds (but not for CoNi(EDTA) · $6H_2O$ and CoCu(EDTA) · $6H_2O$ in which Co(II) is "hydrated") a sharp weight loss appears on TG curves, associated with a definite endothermic effect on DTA curves. These complexes yield M and Co carbonates after pyrolysis (whereas CoNi and CoCu give Co carbonate and Ni or Cu oxide). The observed weight losses (Table 1) approximately fit (except for the CoZn complex *) the elimination of two CO_2 molecules (ca. 1.25 moles for CoZn). This might imply the conversion of both carbonates in protoxides [44]. If so, then it is not surprising that a carbonate mixture (MgCo, MnCo, CoCo) evolves through a different way than that of an oxide and a (cobalt) carbonate (CoNi and CoCu), but it is not easily understandable why other carbonate mixtures (MnNi, MgNi, ZnNi, MnZn, ZnZn) behave differently. Actually, although all the anhydrous carbonates considered here are isostructural in their crystalline phases [45], the fact that the pyrolysis products are practically amorphous precludes simple inferences from that structural similarity. Perhaps, the anomaly for CoZn might be related to the singular (in the present context) behaviour of the Co–Zn–O system [44].

In short, the mechanistic cause of this distinctive behaviour is not well understood. In line with that stated above, a more detailed study on the true nature of these phases is required and we endeavour to clarify it in the course of our current research.

The interest in the $(Co_xNi_{1-x})_{1-y}O$ system has motivated us to approach its preliminary study in more detail. Thus, the thermogravimetric study of the complexes CoCo(EDTA) · $6H_2O$, CoNi(EDTA) · $6H_2O$ and NiNi(EDTA) · $6H_2O$ was repeated, now maintaining the heating until mass constancy, both under a dynamic atmosphere and under an air flux. Likewise, the crystallographic evolution of the resulting phases has been followed

---

* It must be remembered that the CoZn complex is not an "ordered" one and Co^{2+} and Zn^{2+} are distributed randomly among the "chelated" and "hydrated" sites.

TABLE 8

X-ray diffraction pattern data (600°C) for $Co_{2-x}Ni_x(EDTA)\cdot 6H_2O$ compounds

Compound	Air atmosphere		N_2 atmosphere	
	d_{obs}(Å)	Assignment	d_{obs}(Å)	Assignment
CoCo	2.85	Co_3O_4	2.86	Co_3O_4
($x = 0$)	2.46	CoO	2.43	Co_3O_4
	2.44	Co_3O_4	2.13	CoO
	2.33	Co_2O_3	2.02	Co_3O_4
	2.13	CoO	1.65	Co_3O_4
	2.02	Co_3O_4	1.55	Co_3O_4
	1.78	Co_2O_3		
$Co_{1.5}Ni_{0.5}$	2.86	Co_3O_4	2.86	Co_3O_4
($x = 0.5$)	2.45	$NiCoO_2$	2.44	$NiCoO_2$
	2.43	Co_3O_4	2.43	Co_3O_4
	2.12	$NiCoO_2$	2.12	$NiCoO_2$
	1.50	$NiCoO_2$	2.03	Ni
CoNi	2.44	$NiCoO_2$	2.44	$NiCoO_2$
$x = 1$)	2.41	NiO	2.43	Co_3O_4
	2.14	CoO	2.11	$NiCoO_2$
	2.11	$NiCoO_2$	2.03	Ni
	2.09	NiO		
	1.49	$NiCoO_2$		
$Co_{0.5}Ni_{1.5}$	2.41	NiO	2.41	NiO
($x = 1.5$)	2.11	$NiCoO_2$	2.11	$NiCoO_2$
	2.09	NiO	2.09	NiO
	2.03	Ni	2.03	Ni
	1.76	Ni	1.76	Ni
	1.48	Ni		
	1.21	NiO		
NiNi	2.41	NiO	2.41	NiO
($x = 2$)	2.09	NiO	2.09	NiO
	2.03	Ni	2.03	Ni
	1.76	Ni	1.76	Ni
	1.48	NiO		
	1.25	Ni		

(using the variable temperature device of the X-ray diffractometer) for samples whose molar Co/Ni ratio range from 2Co/0Ni (CoCo(EDTA) · $6H_2O$) until 0Co/2Ni (NiNi(EDTA) · $6H_2O$) (Table 8).

Under N_2 atmosphere, TG–DTA curves show: (1) in all three cases, the weight loss ends at ca. 1000°C; (2) the observed total weight losses indicate that the ultimate products are the proper metals; (3) the decomposition of the pyrolysis products is endothermic and occurs smoothly (except for the CoCo(EDTA) · $6H_2O$ complex for which the step $CoCO_3 \rightarrow CoO + CO_2$ is clearly distinguishable (ca. 430–550°C) on the curves, but then also evolves smoothly to give Co at 1185°C); (4) the final temperatures are too low to consider a thermal reduction of the oxides [46]. Rather, it would be attributable to the action of some of the EDTA reductor degradation products (CO, CH_4, etc.) * [32,46].

Under an atmosphere of air, the evolution is somewhat different and mass constancy is attained at appreciably lower temperatures (ca. 600°C). After pyrolysis, which concludes at ca. 400°C, a slight (ca. 2%) mass increase is observed before its final stabilization. The total weight losses correspond well with oxide formation. So it follows that: (1) for the CoCo system: $\Delta m_{exp} = 58.4\%$, close to $\Delta m(2/3Co_3O_4) = 60.5\%$, $\Delta m(Co_2O_3) = 59.1\%$ and $\Delta m(2CoO) = 63.1\%$; (2) for CoNi systems: $\Delta m_{exp} = 61.0\%$, $\Delta m(1/3Co_3O_4 + NiO) = 61.8\%$, but $\Delta m(CoO + NiO) = 63.1\%$; (3) for NiNi systems: $\Delta m_{exp} = 62.3\%$, $\Delta m(NiO) = 63.2\%$, $\Delta m(Ni) = 71.1\%$. The fact that the weight losses at ca. 400°C (final pyrolysis) are somewhat higher than in theory, could be attributed to partial reduction and/or non-stoichiometric oxide formation (in the presence of the reductor products of the EDTA pyrolysis). The subsequent mass increase (O_2 uptake) would be then related with the formation of the phases which are stable at these temperatures. This observed double effect ** (partial reduction–oxidation) agrees with the observations of Bhat and Krishna [32] for the acid EDTA complexes of these same metals, $H_2Co(EDTA) \cdot 3H_2O$ and $H_2Ni(EDTA) \cdot 1H_2O$, differing with those reported by Morris et al. [47].

It is of note that the results based on only the experimental weight losses are not, in general, unambiguous. We have summarized in Table 8 the X-ray diffraction data (600°C) corresponding to the different samples (under N_2 and air, respectively). Besides the immediate phases identification, the following more remarkable facts can be mentioned: (1) Ni(s) is detected: (a) in air for Ni/Co ratio in the samples higher than 1/1; (b) in N_2 atmosphere for all the samples containing Ni(II); (2) as the Ni content in the samples increases, Co(III) (Co_2O_3 and/or Co_3O_4) becomes destabilized with respect to a protoxide solid solution formation ($NiCoO_2$). The fact that for the CoNi compound the Co_3O_4 spinel can still be detected precisely in the non-oxidant N_2 atmosphere can be related to the lack of enough NiO to stabilize CoO (due to the reduction $NiO \rightarrow Ni$). (3) Unlike that observed in air, the Co_2O_3 phase is not detected for the CoCo complex under N_2 atmosphere.

These results are then consistent with the thermogravimetric data and also with the literature [18,44].

---

* Although a N_2 flux is maintained, the muffle design implies that the total pulling of the gases should take a relatively long period.

** An analogous effect is observed when the experiments under N_2 atmosphere are performed without the previous total evacuation of the muffle.

On the other hand, it must be emphasized that the X-ray patterns of samples having a ratio Ni/Co $\geqslant 1$, heated at 400°C (under N_2 atmosphere), indicates clearly the presence of NiO (if poorly crystallized). This result supports the above proposed mechanism for the ligand pyrolysis.

The agreement with the expectations from the literature allows one to consider these results as confirming the EDTA derivatives as potentially suitable complex oxide precursors. This suitability will depend lastly on the surface characteristics of the resulting phases which in turn will control their catalytic properties.

CONCLUSIONS

It seems clear that the thermodynamic "occupational preference" showed by the isostructural $MM'(EDTA) \cdot 6H_2O$ materials [2], controlling the relative disposition of the metallic cations, has further consequences and determines the observed type of thermal behaviour. This fact suggests that it would be possible to alter the degradation pattern (and very likely the final products) for a given M/M′ couple selecting an adequate EDTA-like ligand. An analogous study to that reported here dealing with CDTA derivatives (in which the "occupational preference" has kinetic origin [12]) is now in progress and might offer comparative clarifying results.

On the other hand, the elucidation of the observed peculiar behaviour remains as an open question for the complexes having Co^{2+} (in the "chelated" site) after the ligand pyrolysis. This is a key question of our current research intended to gain more insight on the nature and properties of the degradation products.

ACKNOWLEDGEMENTS

Grateful acknowledgement is made to the CAICYT for partial support of this research under Grant No. 2930/83. J.V.F. thanks the Spanish Ministerio de Educación y Ciencia for a F.P.I. fellowship.

REFERENCES

1 E. Escrivá, D. Beltrán and J. Beltrán, An. Quim., B77 (1981) 330.
2 E. Escrivá, A. Fuertes and D. Beltrán, Transition Met. Chem., 9 (1984) 184 and references therein.
3 A.I. Pozhidaev, T.N. Polynova, M.A. Porai-Koshits and N.N. Neronova, Zh. Strukt. Khim., 14 (1973) 570.
4 E.F.K. McCandlish, T.K. Michael, J.A. Nael, E.C. Lingafelter and N.J. Rose, Inorg. Chem., 17 (1978) 1383.
5 D. Beltrán, E. Escrivá and M. Drillon, J. Chem. Soc. Faraday Trans. 2, 78 (1982) 1733.
6 M. Drillon, E. Coronado, D. Beltrán and R. Georges, Chem. Phys., 79 (1983) 449; J. Appl. Phys., 57 (1985) 3353.

7 M. Drillon, E. Coronado, D. Beltrán, J. Curely, R. Georges, P.R. Nugteren, L.J. de Jongh and J.L. Genicon, J. Mag. Mag. Mat., 54–57 (1986) 1507.
8 E. Coronado, M. Drillon, A. Fuertes, D. Beltrán, A. Mosset and J. Galy, J. Am. Chem. Soc., 108 (1986) 900.
9 A. Mosset, J. Galy, E. Coronado, M. Drillon and D. Beltrán, J. Am. Chem. Soc., 106 (1984) 2864.
10 E. Coronado, M. Drillon, D. Beltrán and J.C. Bernier, Inorg. Chem., 23 (1984) 4000.
11 E. Coronado, M. Drillon, D. Beltrán, A. Mosset and J. Galy, J. Phys., 46 (1985) c8.
12 A. Fuertes, C. Miravitlles, E. Escrivá, E. Martinez-Tamayo and D. Beltrán, Transition Met. Chem., 10 (1985) 432.
13 A. Fuertes, C. Miravitlles, E. Escrivá, E. Coronado and D. Beltrán, J. Chem. Soc. Dalton Trans., in press.
14 A. Fuertes, C. Miravitlles, E. Molins, E. Escrivá and D. Beltrán, Acta Crystallogr., in press.
15 K. Vidyasagar, J. Gopalakrishnan and C.N.R. Rao, Inorg. Chem., 23 (1984) 1206.
16 D.R. Glasson, J. Appl. Chem., 13 (1963) 124; 14 (1964) 121.
17 R.C. Mehrotra and R. Bohra, Metal Carboxylates, Academic Press, London, 1983, p. 121.
18 S. Boskovic, S. Malcic and M. Stevanovic, Trans. J. Br. Ceram. Soc., 75 (5) (1976) 107.
19 J. Burzlagg, V. Bohme and M. Gomm, DISTAN 1977, University of Erlangen, Erlangen, F.R.G., 1977.
20 V.A. Logvinenko and M.L. Myachina, J. Therm. Anal., 19 (1980) 45.
21 M. Falk and O. Knop, in F. Franks (Ed.), Water: A Comprehensive Treatise, Vol. 2, Plenum Press, New York, Chap. 2.
22 R.H. Nuttall and D.M. Stalker, J. Inorg. Nucl. Chem., 40 (1978) 39.
23 R.S. Drago, Physical Methods in Chemistry, W.B. Saunders, Philadelphia, PA, 1977.
24 J. Paulik, F. Paulik and V. Logvinenko, J. Therm. Anal., 10 (1976) 123.
25 E. Martínez-Tamayo, A. Beltrán-Porter and D. Beltrán-Porter, Thermochim. Acta, 98 (1986) 167.
26 E. Martínez-Tamayo, A. Beltrán-Porter and D. Beltrán-Porter, Thermochim. Acta, 98 (1986) 175.
27 R.R.A. Abou-Shaaban and P. Simonelli, Thermochim. Acta, 26 (1978) 67; 26 (1978) 89.
28 V. Satava. Thermochim. Acta, 2 (1971) 423.
29 S.F. Hulbert, J. Br. Ceram. Soc., 8 (1969) 11.
30 C. Duval, Anal. Chim. Acta, 16 (1957) 545.
31 W.W. Wendlandt, Anal. Chim. Acta, 32 (1960) 848.
32 T.R. Bhat and R. Krishna, J. Inorg. Nucl. Chem., 29 (1967) 179.
33 G.I. Vorobiev, Russ. J. Inorg. Chem., 15 (1970) 1371.
34 L.I. Martynenko, Russ. J. Inorg. Chem., 12 (1967) 218.
35 V.A. Logvinenko and A.K. Nikolaev, Izv. Sib. Otd. Akad. Nauk. URSS, 11 (1966) 100; H.G. Wiedemann (Ed.), Thermal Analysis, Vol. 2, Proc. III ICTA, Birkhäuser Verlag, Basel, 1972, p. 779.
36 R.G. Charles, J. Inorg. Nucl. Chem., 28 (1966) 407.
37 C.W. Beck. Ph. D. Thesis, Harvard University, MA, 1946; Am. Mineral., 35 (1950) 985.
38 S.R. Mohanty and N.M. Ray, Indian J. Chem., 3 (1965) 37.
39 D. Beltrán, Ph. D. Thesis, Universidad de Valencia, Spain, 1974.
40 B.J. Hathaway and D.E. Billing, Coord. Chem. Rev., 5 (1970) 143.
41 X. Solans, M. Font-Altaba, J. Oliva and J. Herrera, Acta Crystallogr., 39 (1983) 435.
42 F. Feigl, Spot Test in Inorganic Analysis, Elsevier, Amsterdam, 1958, p. 385.
43 V.G. Keramides and W.B. White, J. Am. Ceram. Soc., 57 (1974) 22.
44 J. Robin, Ann. Chim., 10 (1955) 389.
45 R.W.G. Wyckoff, Crystal Structures, Vol. 2, 2nd edn., Interscience, New York, 1964, p. 362.
46 P. Pascal, Nouveau Traité de Chimie Minérale, Vol. XVIII, Masson et Cie., Paris, 1963.
47 M.L. Morris, R.W. Dunham and W.W. Wendlandt, J. Inorg. Nucl. Chem., 20 (1961) 274.